◆ Human Brain Mapping 31:1900–1906 (2010) ◆

Evidence for Retrochiasmatic Tissue Loss in Leber's Hereditary Optic Neuropathy

Valeria Barcella,[1,2] Maria A. Rocca,[1,2] Stefania Bianchi-Marzoli,[3] Jacopo Milesi,[3] Lisa Melzi,[3] Andrea Falini,[4] Luisa Pierro,[3] and Massimo Filippi[1,2]*

[1]*Neuroimaging Reseach Unit, Institute of Experimental Neurology, Scientific Institute and University Ospedale San Raffaele, Milan, Italy*
[2]*Department of Neurology, Scientific Institute and University Ospedale San Raffaele, Milan, Italy*
[3]*Department of Ophthalmology, Scientific Institute and University Ospedale San Raffaele, Milan, Italy*
[4]*Department of Neuroradiology, Scientific Institute and University Ospedale San Raffaele, Milan, Italy*

Abstract: Patients with Leber's hereditary optic neuropathy (LHON) have loss of central vision with severe damage of small-caliber fibers of the papillomacular bundle and optic nerve atrophy. The aim of this study was to define the presence and topographical distribution of brain grey matter (GM) and white matter (WM) injury in LHON patients using voxel-based morphometry (VBM). The correlation of such changes with neuro-ophthalmologic findings and measurements of peripapillary retinal nerve fiber layer (RNFL) thickness by optical coherence tomography (OCT) was also assessed. Dual-echo and fast-field echo scans were acquired from 12 LHON patients and 12 matched controls. VBM analysis was performed using SPM5 and an ANCOVA model. A complete neuro-ophthalmologic examination, including standardized automated Humphrey perimetry as well as average and temporal peripapillary RNFL thickness measurements were obtained in all the patients. Compared with controls, average peripapillary RNFL thickness was significantly decreased in LHON patients. LHON patients also had significant reduced GM volume in the bilateral primary visual cortex, and reduced WM volume in the optic chiasm, optic tract, and several areas located in the optic radiations (OR), bilaterally. Visual cortex and OR atrophy were significantly correlated with average and temporal peripapillary RNFL thickness ($P < 0.001$; r values ranging from 0.76 to 0.89). Brain damage in patients with LHON is not limited to the anterior visual pathways, but extends posteriorly to the OR and the primary visual cortex. Such a damage to the posterior parts of the visual pathways may be due either to trans-synaptic degeneration secondary to neuroaxonal damage in the retina and optic nerve or to local mitochondrial dysfunction. *Hum Brain Mapp 31:1900–1906, 2010.*

Key words: Leber's hereditary optic neuropathy; retinal nerve fiber layer thickness; optical coherence tomography; voxel-based morphometry

INTRODUCTION

The clinical hallmark of Leber's hereditary optic neuropathy (LHON), a mitochondrial disorder mainly affecting males [Huoponen et al., 1991; Newman et al., 1991; Wallace et al., 1988], is a loss of central vision, which is almost always bilateral and severe [Johns et al., 1992; Riordan-Eva et al., 1995]. Pathologically, LHON is characterized by a degeneration of the retinal ganglion cell layer and optic nerve axons, with a selective loss of the smaller-caliber

*Correspondence to: Massimo Filippi, Neuroimaging Research Unit, Institute of Experimental Neurology, Scientific Institute and University Ospedale San Raffaele, Via Olgettina, 60, 20132 Milan, Italy. E-mail: m.filippi@hsr.it

Received for publication 9 September 2009; Revised 1 December 2009; Accepted 3 December 2009

DOI: 10.1002/hbm.20985

Published online 13 May 2010 in Wiley Online Library (wileyonlinelibrary.com).

fibers of the papillomacular bundle since the early stage of the disease [Sadun et al., 2000]. Optical coherence tomography (OCT) is a noninvasive technique that can be used to measure peripapillary retinal nerve fiber layer (RNFL) thickness, which was found to be reduced in patients with LHON particularly in the temporal side [Savini et al., 2005]. Consistent with such clinical and pathological features, magnetic resonance imaging (MRI) studies have demonstrated atrophy and increased T2-weighted signal in the optic nerves from LHON patients [Kermode et al., 1989; Morrissey et al., 1995]. Although an increased prevalence of multiple sclerosis-like lesions has been reported in LHON patients [Harding et al., 1992], it is still unclear whether and to what degree the central nervous system (CNS) is damaged in patients with LHON. *Postmortem* [Wilson, 1963], neurophysiologic [Howell, 1998], and quantitative MR [Inglese et al., 2001a] studies support the notion of a selective and isolated involvement of the optic nerve in this disease. On the contrary, a few preliminary MR spectroscopy (MRS) studies have shown an abnormal mitochondrial energy metabolism in the occipital lobe from these patients [Barbiroli et al., 1995; Cortelli et al., 1991; Lodi et al., 2002].

Recently, several approaches have been developed to obtain measures of brain tissue loss at a regional level [Benedict et al., 2005; Carone et al., 2006; Pagani et al., 2007; Sailer et al., 2003]. The application of such approaches is contributing remarkably to the identification of the topography of CNS involvement in many neurological conditions [Bermel and Bakshi, 2006; Bozzali et al., 2008]. In this context, voxel-based morphometry (VBM) is a fully automated and accurate method that allows comparison of local volumes of grey matter (GM) and white matter (WM) between groups of subjects [Ashburner and Friston, 2000]. To the best of our knowledge, no study has addressed yet the distribution of GM and WM loss in patients with LHON and, more importantly, whether trans-synaptic degeneration phenomena do occur with involvement of the retrochiasmatic visual structures in these patients. To this aim, we used MRI and VBM to assess in a cohort of LHON patients the topography of GM and WM volume changes, as well as to investigate whether they are correlated with clinical and OCT measures for peripapillary RNFL thickness.

MATERIALS AND METHODS

Subjects

To be included, patients had to carry one of the three primary mitochondrial DNA (mtDNA) mutations associated with LHON. In addition, patients had to have a normal neurological examination and no other ophthalmic diseases (apart from sequelae secondary to optic nerve involvement) as well as no previous history or presence of other neurological, psychiatric, and major medical conditions, or substance abuse.

We studied 12 patients with LHON (nine men, three women, five patients had 11,778, four 3,460, and three 14,484 mtDNA mutation) recruited from the Neuro-Ophthalmology Clinic at San Raffaele Scientific Institute, Milan, Italy. Their mean age was 33.6 years (range = 20–60 years) and their median disease duration was 8.2 years (range = 1–23 years). Twelve sex- and age-matched healthy subjects, with no history of previous neurological and ophthalmologic disorders served as controls (nine men and three women; mean age = 33.2 years, range = 23–58 years). Approval from the local Ethics Committee and written informed consent from all subjects were obtained before study initiation.

Neuroophthalmologic Assessment

Before MRI acquisition, each patient underwent a neuroophthalmologic examination, including standardized automated perimetry (Humphrey Zeiss, 30-2 SITA standard program). Quantitative measurement used for statistical comparisons were LogMar visual acuity (VA) and Humphrey Mean Deviation (MD). Quantitative peripapillary RNFL thickness measurements were obtained using a commercially available optical coherence tomographer (Stratus OCT, Carl Zeiss Ophthalmic Systems, fast RNFL thickness 3.4). Pupil dilatation was induced in all patients, and an internal fixation was used whenever possible. For each eye, we measured the average peripapillary RNFL thickness (360° measure), and the temporal quadrant RNFL thickness (316°–45° unit circle). The OCT software uses an automated computerized algorithm to rank the RNFL thickness measurements from each patients' eye against a normal percentile distribution derived from a database of age-matched control subjects. For this reason, OCT was not obtained from the healthy controls of this study.

MRI Acquisition

Using a 3.0 T scanner (Intera, Philips Medical Systems, Best, The Netherlands), the following sequences of the brain were obtained from all subjects: (1) dual-echo turbo spin echo (TSE), (TR = 3,500 ms, TE = 24/120 ms; echo train length = 5; flip angle = 150°, 44 contiguous, 3-mm-thick, axial slices with a matrix size = 256 × 256 and a field of view [FOV] = 240 × 240 mm^2); and (2) 3D T1-weighted fast field echo (FFE), (TR = 25 ms, TE = 4.6 ms, flip angle = 30°, 220 contiguous, axial slices with voxel size = 0.89 × 0.89 × 1 mm^3, matrix size = 256 × 256, FOV = 230 × 230 mm^2).

Image Analysis and Postprocessing

WM hyperintensities (WMHs), if any, were identified by an experienced observer (AF) on dual-echo scans.

TABLE I. Retinal nerve fiber layer thickness values (μm) in patients with Leber's hereditary optic neuropathy

RNFL thickness	Left eye	Right eye
Average (SD) (number of abnormal eyes[a])	55.4 (15.1) (12)	57.1 (15.8) (12)
Temporal (SD) (number of abnormal eyes[a])	44.8 (17.6) (12)	48.7 (20.2) (12)

Abbreviations: RNFL = retinal nerve fiber layer, SD = standard deviation.
[a]Below normal (<5th percentile) as compared with a database of age-matched control subjects. See text for further details.

VBM analysis was performed using the SPM5 software (http://www.fil.ion.ucl.ac.uk/spm). First, MR images were segmented into GM, WM, and cerebrospinal fluid by using the standard unified segmentation model in SPM5 [Ashburner and Friston, 2005]. To remove nonbrain tissue, the "clean-up" procedure was applied to the segmented GM images. Then, GM and WM segmented images were normalized, respectively, to the GM and WM population templates generated from the complete image set using the Diffeomorphic Anatomical Registration using Exponentiated Lie algebra (DARTEL) registration method [Ashburner, 2007]. This nonlinear warping technique minimizes between-subject structural variations. The final voxel resolution after DARTEL was $1.5 \times 1.5 \times 1.5$ mm^3. Spatially normalized images were then modulated to ensure that the overall amount of each tissue class was not altered by the spatial normalization procedure, and smoothed with a 8-mm full-width at half-maximum Gaussian kernel.

Statistical Analysis

The smoothed GM and WM images were analyzed in a multiple regression design. Age, gender, and total intracranial volume (ICV), measured with SPM5, were entered into the design matrix as nuisance variables. Regional differences in GM and WM volumes were assessed using the general linear model and the significance of each effect was determined by using the theory of Gaussian fields [Friston et al., 1995]. GM and WM differences were assessed at a corrected statistical threshold of $P < 0.05$ (family wise error—FWE). The location of clusters of significant WM changes in the WM fiber bundles of interest was defined using the anatomical probabilistic maps of Burgel et al. [2006] and available in the SPM Anatomy toolbox (http://www.fz-juelich.de/ime/spm_anatomy_toolbox). A linear regression analysis was used to assess the correlations between regional damage and clinical (disease duration, VA, MD) and OCT (average and temporal RNFL thickness) findings. For the correlation analysis, two statistical analyses were run. First, we performed a whole-brain analysis, in which we accepted a conservative level of significance of $P < 0.05$ corrected for multiple comparisons. Since this analysis did not show any region with a significant correlation, based on the results of the between-group comparisons of GM and WM volume changes and of previous phosphorus[31] MRS studies [Barbiroli et al., 1995; Cortelli et al., 1991; Lodi et al., 2002], we restricted our analysis to those regions along the visual pathways which showed significant volume difference between LHON patients and controls. To this aim, a mask including these regions was created from the contrast assessing between-group differences and applied to the SPM correlation analysis using WFU Pickatlas [Maldjian et al., 2003]. For this second, a priori based analysis, we accepted a less stringent level of significance of $P < 0.001$, uncorrected.

A paired t test was used to compare neuroophthalmologic quantities derived from the left and right eyes.

RESULTS

Neuroophthalmologic Assessment

At the time of evaluation, all the LHON patients had bilateral optic nerve involvement. LogMAR VA was decreased in 22 affected eyes, while normal logMAR VA was found in two affected eyes (mean LogMAR VA: right eye = 0.49, left eye = 0.60, range from 3 to 0). Average MD was −16.3 dB (range: −33.4; −1.5) in the right eye and −16.8 dB (range: −32.6; −2.7) in the left eye.

OCT Findings

Table I reports the mean values of average and temporal peripapillary RNFL thickness measurements obtained in the right and the left eyes of patients with LHON. Peripapillary average RNFL thickness was reduced in all affected eyes. None of the patients had peripapillary RNFL thickness measurements above normal. Figure 1 shows an example of OCT results for RNFL thickness measurements in one LHON patient.

MRI Evaluation

Nonspecific brain T2-hyperintense lesions (less than three lesions with a diameter smaller than 6 mm) were detected in three LHON patients and one healthy control. None of these lesions was located along the optic radiations (OR) or in the occipital cortex. ICV was = 1489.5 ml (SD = 175 ml) in LHON patients and 1510.7 ml (SD = 144 ml) in healthy controls (P = n.s.).

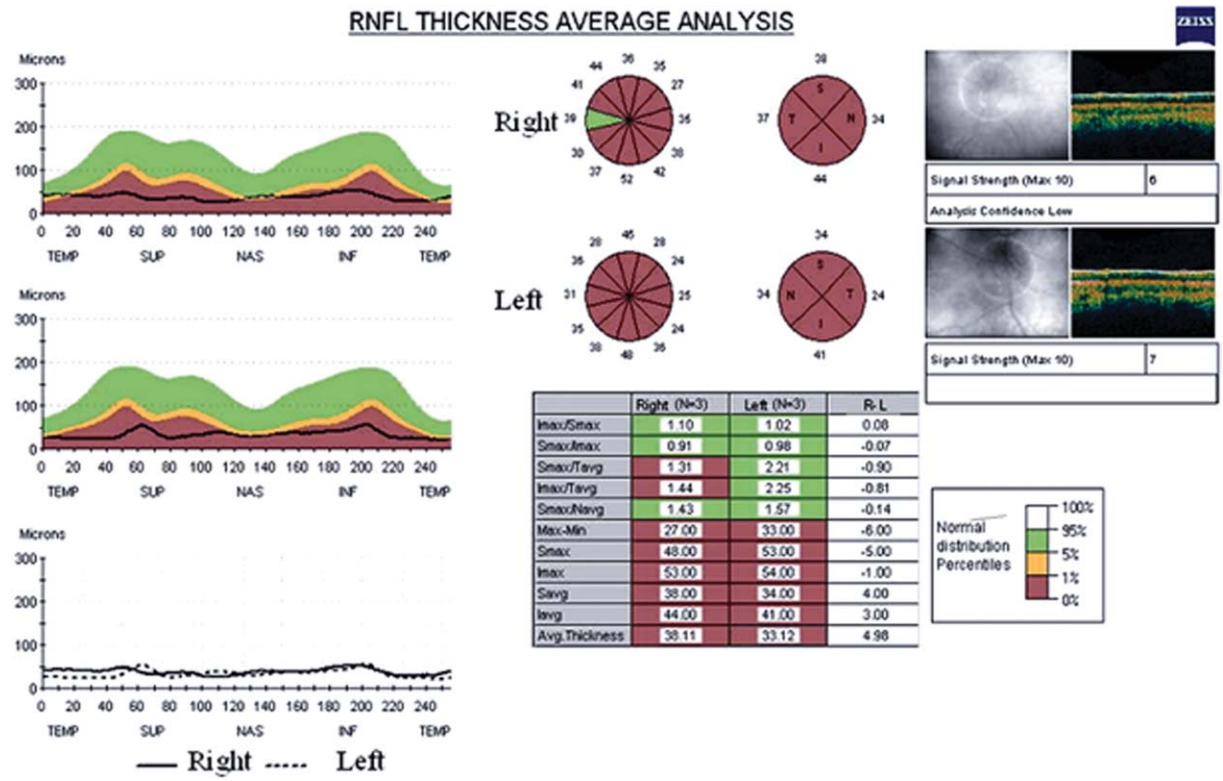

Figure 1.

OCT from a patient with LHON. Graph of retinal nerve fiber layer (RNFL) thickness obtained with optic coherence tomography from a 20-year-old gentleman with Leber's hereditary optic neuropathy and disease duration of 18 months. Measurements below the <5th percentile of the normal distribution are represented in red. In both eyes a significant decrease of average and temporal RNFL thickness is appreciable.

Compared with controls, LHON patients had significant clusters of locally reduced GM volume in the bilateral primary visual cortex (V1) (BA17), (SPM space coordinates: −8, −87, −3; −11, −91, 18, and 13, −81, 1; $P < 0.001$ FWE corrected; see Fig. 2).

Compared with controls, LHON patients had significant clusters of locally reduced WM volume in the chiasm (SPM space coordinates: 7, −3, −14, and −11, −6, −15; $P < 0.001$ FWE corrected), the optic tracts (SPM space coordinates: 22, −21, −9, $P = 0.05$ FWE corrected; and −21, −16, −9, $P = 0.03$ FWE corrected), and several areas located in the ORs (SPM space coordinates: left OR −21, −16, −9, $P = 0.02$ FWE corrected; and −20, −79, 18, $P = 0.01$ FWE corrected; right OR 22, −22, −8, $P = 0.002$ FWE corrected; and 30, −82, 1, $P = 0.01$ FWE corrected; see Fig. 3).

Correlations Between Neuroophthalmologic, OCT, and MRI Findings

Since no statistically significant differences were found for neuroophthalmologic measures (VA, MD) or OCT peripapillary RNFL thickness values between right and left eyes in patients with LHON, their mean values were used to assess correlations. In patients with LHON, significant correlations ($P < 0.001$, uncorrected) were found between:

- left V1 tissue loss vs. reduction of average peripapillary RNFL thickness (r 0.89), and temporal RNFL thickness (r 0.76);
- right V1 tissue loss vs. reduction of temporal RNFL thickness (r 0.89)
- right OR tissue loss vs. reduction of average peripapillary RNFL thickness (r 0.78);
- left OR tissue loss vs. reduction of average peripapillary RNFL thickness (r 0.84), and temporal RNFL thickness (r 0.79).

No correlation was found between MRI findings and disease duration, VA and MD.

DISCUSSION

In this study, we used MRI and VBM to define the regional distribution of CNS tissue loss in affected patients

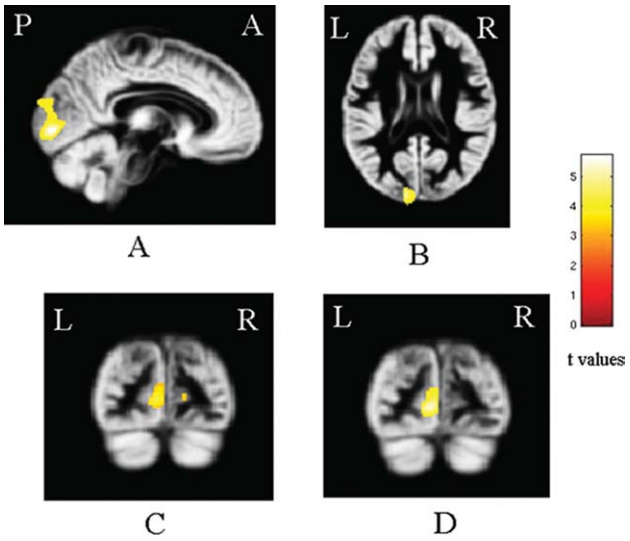

Figure 2.

GM loss in LHON. Statistical parametric mapping regions of grey matter (GM) loss in patients with Leber's hereditary optic neuropathy vs. controls, superimposed on the customized GM template, at a threshold of $P < 0.05$ corrected for multiple comparisons. Images are in neurological convention.

with LHON. Considering that selective involvement of retinal ganglion cells and optic nerve axons is the main feature of this condition, and that the retina is composed of unmyelinated axons [Frohman et al., 2006; Gordon-Lipkin et al., 2007], our working hypothesis was that LHON patients in a chronic phase of the disease should harbor changes in the visual retrochiasmatic structures, as a consequence of trans-synaptic degeneration, following neuroaxonal damage to the retina and optic nerve.

To assess optic nerve involvement, we used OCT measurements, which allow an estimation of the thickness of peripapillary RNFL. RNFL is made up predominantly by axons before they enter the optic nerve and measures of its thickness can provide a reliable estimate of axonal injury associated with disease [Costello et al., 2006; Savini et al., 2005; Trip et al., 2006]. In agreement with previous studies in patients outside the acute phase of LHON [Barboni et al., 2005; Savini et al., 2005], OCT analysis of our cohort confirmed a significant thinning of the peripapillary RNFL thickness, particularly in its temporal portion of the optic disc. Small fibers on the temporal side of the optic disc have indeed been demonstrated to be the first and the most severely affected by this disease from the subclinical stage [Barboni et al., 2005; Savini et al., 2005]. This finding fits with the notion that an early loss of fibers occurs in the papillomacular bundle, [Sadun et al., 2000] which is reflected clinically by an early deficit of central vision [Carelli et al., 2004; Nikoskelainen et al., 1996].

VBM analysis showed that, compared to healthy controls, patients with LHON experience a significant loss of tissue in the optic pathways, bilaterally, which extends from the optic chiasm, through the optic tracts, and the ORs, to the primary visual cortex. The detection of tissue loss in the optic chiasm and optic tracts in LHON patients is in agreement with the results of a few autopsy studies, which reported destruction of the myelin sheaths and axis cylinders in the fibers subserving macular vision in these structures [Kwittken and Barest, 1958; Wilson, 1963]. Remarkably, we found no GM loss in the lateral geniculate nucleus (LGN), even when the statistical threshold for significance was lowered at a $P < 0.001$, uncorrected. Several factors might contribute to explain such a somewhat unexpected finding. First, we should consider the structure and organization of the LGN, which receives retinofugal projections from both eyes terminating in six distinct layers [Sadun et al., 2000]. In detail, M-type large retinal ganglion cells with large axons project to Layers 1 and 2, whereas P-type small retinal ganglion cells with small axons, which are usually affected in LHON, project to Layers 3 and 6 [Sadun et al., 2000]. As a consequence, it is tempting to speculate that the uneven involvement of nerve fibers in such a relatively small structure might not result in a tissue loss detectable in vivo using MRI and VBM. An alternative, but not mutually exclusive, explanation for the lack of LGN atrophy might be the coexistence in this structure of neurons and axons at different stages of damage. Indeed, neuroaxonal swelling, which may occur during cell death, has the potential to counteract tissue loss secondary to the destruction of a substantial number of neurons and axons. However, the presence of atrophy in the

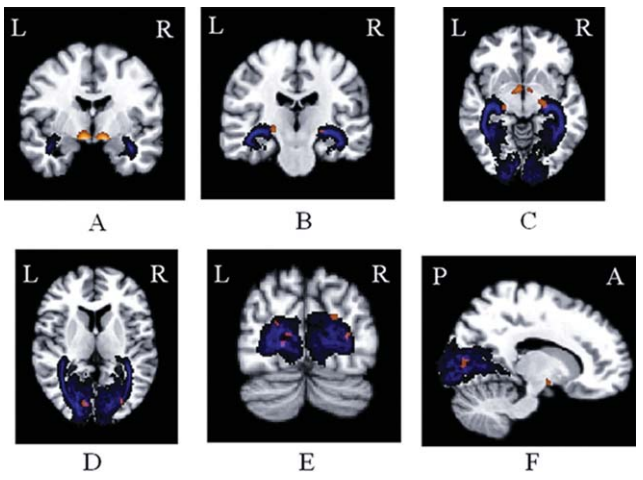

Figure 3.

WM loss in LHON. Clusters of significant white matter (WM) loss (in yellow/red) in patients with Leber's hereditary optic neuropathy superimposed on an anatomical probabilistic map of the optic radiations (OR) available in the SPM Anatomy toolbox (http://www.fz-juelich.de/ime/spm_anatomy_toolbox). Reduced WM volume is visible in the chiasm and in several areas located in the ORs. Images are in neurological convention.

occipital cortex is against this hypothesis. Finally, the size of this structure and its changes in diseased patients might be beyond the resolution of our technique and the statistical threshold we applied. Indeed, we reran our analysis using an uncorrected statistical threshold of $P < 0.01$ (which is usually not advisable for a VBM analysis), and we found significant atrophy in the left LGN. This suggests that the enrolment of a higher number of subjects or the use of a ROI-based approach probably would have allowed us to detect LGN atrophy.

The most intriguing finding of this study is the in vivo demonstration of a significant tissue loss in the ORs and primary visual cortices in LHON patients. This is in agreement with the results of phosphorus[31] MRS studies [Barbiroli et al., 1995; Cortelli et al., 1991; Lodi et al., 2002], which detected metabolic abnormalities in the normal-appearing WM of the occipital lobes from LHON patients and their nonaffected siblings carrying the same mtDNA mutations. On the contrary, another diffusion tensor (DT) and magnetization transfer (MT) MRI study did not detect any microscopic abnormality of the OR and primary visual cortex from 10 LHON patients [Inglese et al., 2001b]. The discrepancy between our results and those of the previous study [Inglese et al., 2001b] are likely due to the fact that the techniques used assessed different aspects of the disease pathology, i.e., tissue loss in our study vs. intrinsic tissue changes in the surviving tissue in that of Inglese et al. [2001b]. For instance, axonal loss in the ORs may be associated with fiber collapsing which would result in atrophy and a "pseudonormalization" of the relative proportion of free and bound water, as measured by MT MRI, and water diffusivity, as measured by DT MRI. In addition, Inglese et al. [2001b] used a region of interest analysis to sample a small portion of the ORs and the primary visual cortex. Since we found a pattern of damage to the ORs and the primary visual cortices consistent with the selective involvement of the papillomacular fibers, it can not be excluded that the placement of the ROI might have biased the results of Inglese et al. [2001b]. Finally, the small sample of subjects studied by Inglese et al. [2001b] is likely to have reduced their statistical power.

OR and visual cortex tissue loss might be secondary to trans-synaptic degeneration, which in turn may follow neuroaxonal damage to the retina and optic nerve. Admittedly, we can not rule out completely subclinical tissue changes in the brain due to the presence of mitochondrial mutations. To this end, future studies should be performed to contrast LHON with other conditions (i.e., ischemic optic neuropathy or traumatic optic neuropathy), where an isolated optic nerve involvement is likely to be present. However, the notion that such a damage might cause dystrophic changes in the neurons and pathways projecting to the LGN and then to the primary visual cortices is in line with the results of previous quantitative MR studies conducted in patients with optic neuritis [Audoin et al., 2006], where significant abnormalities have been detected in these structures. In addition, studies of chronic glaucoma have suggested that damage to retinal ganglion cells may lead to degenerative changes in the LGN and the primary visual cortex [Boucard et al., 2009; Yucel et al., 2003]. Visual cortex atrophy has also been described in patients with retinal degeneration [Boucard et al., 2009] and albinism [von dem Hagen et al., 2005].

In our study, the hypothesis that retinal and optic nerve damage might cause morphological changes in the ORs and the primary visual cortices is partially supported by the correlation we found between RNFL thickness and VBM quantities. Clearly, considering the relatively small number of patients included, such as analysis did not allow us to discriminate a clear effect of laterality, as well as the differential effect of each mtDNA mutation. Remarkably, similarly to the results of a previous study [Inglese et al., 2001b] that found no relationship between the extent of brain microscopic tissue damage, measured using different quantitative MR-based techniques, and disease duration, this analysis did not detect any correlation between VBM findings and disease duration, which, if confirmed, would suggest that such a volume loss may occur in the first year from disease onset, if not already present before it.

In conclusion, our results support previous studies demonstrating that CNS involvement in patients with LHON is not limited to the anterior visual pathways, but rather extends posteriorly to the OR and primary visual cortex, possibly through trans-synaptic degeneration phenomena secondary to neuroaxonal damage to the retina and optic nerve.

REFERENCES

Ashburner J (2007): A fast diffeomorphic image registration algorithm. Neuroimage 38:95–113.

Ashburner J, Friston KJ (2000): Voxel-based morphometry—The methods. Neuroimage 11:805–821.

Ashburner J, Friston KJ (2005): Unified segmentation. Neuroimage 26:839–851.

Audoin B, Fernando KT, Swanton JK, Thompson AJ, Plant GT, Miller DH (2006): Selective magnetization transfer ratio decrease in the visual cortex following optic neuritis. Brain 129:1031–1039.

Barbiroli B, Montagna P, Cortelli P, Iotti S, Lodi R, Barboni P, Monari L, Lugaresi E, Frassineti C, Zaniol P (1995): Defective brain and muscle energy metabolism shown by in vivo 31P magnetic resonance spectroscopy in nonaffected carriers of 11778 mtDNA mutation. Neurology 45:1364–1369.

Barboni P, Savini G, Valentino ML, Montagna P, Cortelli P, De Negri AM, Sadun F, Bianchi S, Longanesi L, Zanini M, et al. (2005): Retinal nerve fiber layer evaluation by optical coherence tomography in Leber's hereditary optic neuropathy. Ophthalmology 112:120–126.

Benedict RH, Zivadinov R, Carone DA, Weinstock-Guttman B, Gaines J, Maggiore C, Sharma J, Tomassi MA, Bakshi R (2005): Regional lobar atrophy predicts memory impairment in multiple sclerosis. AJNR Am J Neuroradiol 26:1824–1831.

Bermel RA, Bakshi R (2006): The measurement and clinical relevance of brain atrophy in multiple sclerosis. Lancet Neurol 5:158–170.

Boucard CC, Hernowo AT, Maguire RP, Jansonius NM, Roerdink JB, Hooymans JM, Cornelissen FW (2009): Changes in cortical grey matter density associated with long-standing retinal visual field defects. Brain 132:1898–1906.

Bozzali M, Cercignani M, Caltagirone C (2008): Brain volumetrics to investigate aging and the principal forms of degenerative cognitive decline: A brief review. Magn Reson Imaging 26:1065–1070.

Burgel U, Amunts K, Hoemke L, Mohlberg H, Gilsbach JM, Zilles K (2006): White matter fiber tracts of the human brain: Three-dimensional mapping at microscopic resolution, topography and intersubject variability. Neuroimage 29:1092–1105.

Carelli V, Ross-Cisneros FN, Sadun AA (2004): Mitochondrial dysfunction as a cause of optic neuropathies. Prog Retin Eye Res 23:53–89.

Carone DA, Benedict RH, Dwyer MG, Cookfair DL, Srinivasaraghavan B, Tjoa CW, Zivadinov R (2006): Semi-automatic brain region extraction (SABRE) reveals superior cortical and deep gray matter atrophy in MS. Neuroimage 29:505–514.

Cortelli P, Montagna P, Avoni P, Sangiorgi S, Bresolin N, Moggio M, Zaniol P, Mantovani V, Barboni P, Barbiroli B, Lugaresi E. (1991): Leber's hereditary optic neuropathy: Genetic, biochemical, and phosphorus magnetic resonance spectroscopy study in an Italian family. Neurology 41:1211–1215.

Costello F, Coupland S, Hodge W, Lorello GR, Koroluk J, Pan YI, Freedman MS, Zackon DH, Kardon RH (2006): Quantifying axonal loss after optic neuritis with optical coherence tomography. Ann Neurol 59:963–969.

Friston KJ, Holmes AP, Poline JB, Grasby PJ, Williams SC, Frackowiak RS, Turner R (1995): Analysis of fMRI time-series revisited. Neuroimage 2:45–53.

Frohman E, Costello F, Zivadinov R, Stuve O, Conger A, Winslow H, Trip A, Frohman T, Balcer L (2006): Optical coherence tomography in multiple sclerosis. Lancet Neurol 5:853–863.

Gordon-Lipkin E, Chodkowski B, Reich DS, Smith SA, Pulicken M, Balcer LJ, Frohman EM, Cutter G, Calabresi PA (2007): Retinal nerve fiber layer is associated with brain atrophy in multiple sclerosis. Neurology 69:1603–1609.

Harding AE, Sweeney MG, Miller DH, Mumford CJ, Kellar-Wood H, Menard D, McDonald WI, Compston DA (1992): Occurrence of a multiple sclerosis-like illness in women who have a Leber's hereditary optic neuropathy mitochondrial DNA mutation. Brain 115 (Part 4):979–989.

Howell N (1998): Leber hereditary optic neuropathy: Respiratory chain dysfunction and degeneration of the optic nerve. Vis Res 38:1495–1504.

Huoponen K, Vilkki J, Aula P, Nikoskelainen EK, Savontaus ML (1991): A new mtDNA mutation associated with Leber hereditary optic neuroretinopathy. Am J Hum Genet 48:1147–1153.

Inglese M, Rovaris M, Bianchi S, Comi G, Filippi M (2001a): Magnetization transfer and diffusion tensor MR imaging of the optic radiations and calcarine cortex from patients with Leber's hereditary optic neuropathy. J Neurol Sci 188:33–36.

Inglese M, Rovaris M, Bianchi S, La Mantia L, Mancardi GL, Ghezzi A, Montagna P, Salvi F, Filippi M (2001b): Magnetic resonance imaging, magnetisation transfer imaging, and diffusion weighted imaging correlates of optic nerve, brain, and cervical cord damage in Leber's hereditary optic neuropathy. J Neurol Neurosurg Psychiatry 70:444–449.

Johns DR, Smith KH, Miller NR (1992): Leber's hereditary optic neuropathy. Clinical manifestations of the 3460 mutation. Arch Ophthalmol 110:1577–1581.

Kermode AG, Moseley IF, Kendall BE, Miller DH, MacManus DG, McDonald WI (1989): Magnetic resonance imaging in Leber's optic neuropathy. J Neurol Neurosurg Psychiatry 52:671–674.

Kwittken J, Barest HD (1958): The neuropathology of hereditary optic atrophy (Leber's disease): The first complete anatomic study. Am J Pathol 34:185–207.

Lodi R, Carelli V, Cortelli P, Iotti S, Valentino ML, Barboni P, Pallotti F, Montagna P, Barbiroli B (2002): Phosphorus MR spectroscopy shows a tissue specific in vivo distribution of biochemical expression of the G3460A mutation in Leber's hereditary optic neuropathy. J Neurol Neurosurg Psychiatry 72:805–807.

Maldjian JA, Laurienti PJ, Kraft RA, Burdette JH (2003): An automated method for neuroanatomic and cytoarchitectonic atlas-based interrogation of fMRI data sets. Neuroimage 19:1233–1239.

Morrissey SP, Borruat FX, Miller DH, Moseley IF, Sweeney MG, Govan GG, Kelly MA, Francis DA, Harding AE, McDonald WI (1995): Bilateral simultaneous optic neuropathy in adults: Clinical, imaging, serological, and genetic studies. J Neurol Neurosurg Psychiatry 58:70–74.

Newman NJ, Lott MT, Wallace DC (1991): The clinical characteristics of pedigrees of Leber's hereditary optic neuropathy with the 11778 mutation. Am J Ophthalmol 111:750–762.

Nikoskelainen EK, Huoponen K, Juvonen V, Lamminen T, Nummelin K, Savontaus ML (1996): Ophthalmologic findings in Leber hereditary optic neuropathy, with special reference to mtDNA mutations. Ophthalmology 103:504–514.

Pagani E, Horsfield MA, Rocca MA, Filippi M (2007): Assessing atrophy of the major white matter fiber bundles of the brain from diffusion tensor MRI data. Magn Reson Med 58:527–534.

Riordan-Eva P, Sanders MD, Govan GG, Sweeney MG, Da Costa J, Harding AE (1995): The clinical features of Leber's hereditary optic neuropathy defined by the presence of a pathogenic mitochondrial DNA mutation. Brain 118 (Part 2):319–337.

Sadun AA, Win PH, Ross-Cisneros FN, Walker SO, Carelli V (2000): Leber's hereditary optic neuropathy differentially affects smaller axons in the optic nerve. Trans Am Ophthalmol Soc 98:223–232; discussion 232–235.

Sailer M, Fischl B, Salat D, Tempelmann C, Schonfeld MA, Busa E, Bodammer N, Heinze HJ, Dale A (2003): Focal thinning of the cerebral cortex in multiple sclerosis. Brain 126:1734–1744.

Savini G, Zanini M, Carelli V, Sadun AA, Ross-Cisneros FN, Barboni P (2005): Correlation between retinal nerve fibre layer thickness and optic nerve head size: An optical coherence tomography study. Br J Ophthalmol 89:489–492.

Trip SA, Schlottmann PG, Jones SJ, Li WY, Garway-Heath DF, Thompson AJ, Plant GT, Miller DH (2006): Optic nerve atrophy and retinal nerve fibre layer thinning following optic neuritis: Evidence that axonal loss is a substrate of MRI-detected atrophy. Neuroimage 31:286–293.

von dem Hagen EA, Houston GC, Hoffmann MB, Jeffery G, Morland AB (2005): Retinal abnormalities in human albinism translate into a reduction of grey matter in the occipital cortex. Eur J Neurosci 22:2475–2480.

Wallace DC, Singh G, Lott MT, Hodge JA, Schurr TG, Lezza AM, Elsas LJ II, Nikoskelainen EK (1988): Mitochondrial DNA mutation associated with Leber's hereditary optic neuropathy. Science 242:1427–1430.

Wilson J (1963): Leber's hereditary optic atrophy: Some clinical and aetiological considerations. Brain 86:347–362.

Yucel YH, Zhang Q, Weinreb RN, Kaufman PL, Gupta N (2003): Effects of retinal ganglion cell loss on magno-, parvo-, koniocellular pathways in the lateral geniculate nucleus and visual cortex in glaucoma. Prog Retin Eye Res 22:465–481.